



Undoped CuO deposited by Spray Pyrolysis technique

F.Z. Chafi^{1*}, A. Hadri¹, C. Nassiri¹, B. Fares¹, L. Laanab¹, N. Hassanain¹, A. Mzerd¹

¹ Physics department Faculty of Science, Mohammed V University, Rabat, Morocco

Received 04 Jan 2015, Revised 21 Nov 2015, Accepted 30 Nov 2015

*Corresponding author: E-mail: chafifatimazahra@gmail.com (F.Z. Chafi); Phone: +212 6 6725 2017

Abstract

In this study undoped copper oxide CuO thin films were deposited on heated glass substrate by using a simple and low cost spray pyrolysis technique. An aqueous solution with different molar concentrations of copper (II) chloride dehydrates ($\text{CuCl}_2 \cdot 2\text{H}_2\text{O}$) as precursor was used. The as-deposited thin films were carried out at fixed substrate temperature of 350°C . The structural, textural and optical properties of the films were determined respectively by X-Ray Diffraction method, Atomic Force Microscopy and UV-Visible Spectrophotometer. The X-Ray Diffraction spectra showed that all samples exhibit polycrystalline nature corresponding to monoclinic crystal structure with two preferred orientations along the (-111) and (111) axis. Polycrystalline morphology with a pyramidal crystallite size depending on the molar concentration of copper (II) chloride dehydrate ($\text{CuCl}_2 \cdot 2\text{H}_2\text{O}$) in starting solution, was observed. Roughness parameters Ra and Rms of the surface and the grain size were investigated as a function of molar concentration. Transmission values varying from 60 to 70% at different molar concentrations were obtained in the wavelength range between 400 and 1200nm.

Keywords: Copper Oxide, thin film, Spray Pyrolysis, molar concentration, XRD, AFM, roughness, transmission

1. Introduction

Copper oxide CuO p-type semiconductor is having drawn a continually increasing interest in the past few years due to their fundamental properties. Indeed, with a stable band gap of $E_g = 1.2 \text{ eV}$ [1, 2, 3], no toxicity properties and relative abundance CuO was considered as an interesting material for a wide array of applications such as heterogeneous catalysts for several environmental processes [4 - 8], solid-state gas sensor heterocontacts [9 - 15], and microwave dielectric materials [16 - 17]. Their use in power sources was received special attention. Thus, in addition to photovoltaic devices [18 - 19], copper oxides were used as an electrode material for lithium batteries and as cathodes in lithium primary cells [20].

In the last decade various CuO structure were produced in different sizes and morphologies, such as, leaf shape, nanoflower, nanotube [21 - 28], microsphere aggregate and other one.

In this work, we report the preparation and characterization of polycrystalline CuO thin films by spraying an aqueous solution of copper (II) chloride dehydrate ($\text{CuCl}_2 \cdot 2\text{H}_2\text{O}$) as a simple preparation method that requires low cost equipment [29]. X-Ray Diffraction (XRD), Atomic Force Microscopy and UV-Visible spectrophotometer were respectively used for characterization. In addition, a specific attention was paid to the influence of the molar concentration of copper (II) chloride dehydrate ($\text{CuCl}_2 \cdot 2\text{H}_2\text{O}$) in the starting solution, on the structural, morphological and optical properties of the sprayed CuO thin films.

2. Experimental

2.1. Preparation of polystructure thin films

The Copper oxide CuO thin films were deposited using a typical spray pyrolysis coating system showed schematically in figure 1. The used starting solution was prepared by dissolving copper (II) chloride dehydrate ($\text{CuCl}_2 \cdot 2\text{H}_2\text{O}$) as precursor in deionized water. This solution with different molar concentrations 0.05M, 0.058M and 0.1M was sprayed into fine droplets using air as a carrier gas on glass substrates heated at fixed temperature of 350°C . Before the deposition of films, glass substrates were cleaned and placed then on the hot

plate. To prevent rapid reduction in the hot plate temperature, spraying was done in short time intervals. All experiments were done under approximately similar conditions.

- 1- Extractor,
- 2- Hot plate,
- 3- Temperature controller,
- 4- Substrates,
- 5- Jet,
- 6- Solution,
- 7- Dosing pump,
- 8- Drive system,
- 9- Drive motor,
- 10- Air pump,
- 11- Thermocouple,

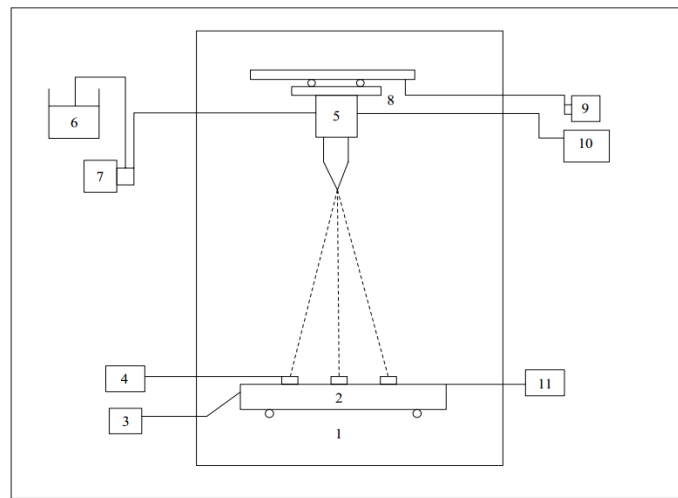


Figure 1: Spray Pyrolysis System

2.2. Structural, morphological and optical characterization of thin films

2.2.1. Structural characterization XRD

X-Ray Diffraction (XRD) patterns of undoped CuO films were recorded by D8 Advance Bruker system using Cu K α ($\lambda = 0.154056$ nm) radiation with 2θ in the range $10^\circ - 60^\circ$. The average crystalline grain size was calculated using the Scherrer's formula (1) based on the XRD patterns:

$$D = K \lambda / (\Delta (2\theta) \cos (\theta)) \quad (1)$$

Where D is the average crystalline (grain) size, K is a constant (~ 1), λ is the X-ray wavelength, $\Delta (2\theta)$ is the full width at half maximum (FWHM) of XRD peaks and θ is the Bragg angle.

The lattice parameters were calculated from the Bragg Formula (2) by calculating the interplanar distance:

$$2 d \sin\theta = n \cdot \lambda \quad (2)$$

Where d is the interplanar distance, θ is the Bragg angle, n is diffraction pattern (whole number) and λ is the wavelength.

2.2.2. Morphological characterization AFM

The Atomic Force Microscopy (AFM) measurements characterize the surface topology of material and provide information in particular on the surface roughness and the grain size of the material studied.

The roughness is the change in height relative to the average height of the surface allows for quantitative measurement of the surface. There are two ways to measure the roughness:

First way is the average deviation of all points of the roughness profile with respect to an average line length of the evaluation:

$$R_a = \sum_i z_i / n \quad (3)$$

Second way is Roughness Mean Square RMS or quadratic roughness. A change in the Rms of the surface can be performed by calculating the standard deviation of the height of each point of the surface z (x, y) by the formula:

$$R_{ms} = \sqrt{\frac{\sum_i z_i^2}{n}} \quad (4)$$

2.2.3. Optical transmission characterization

A Lambda 900 UV/VIS/NIR spectrophotometer was used to determine the optical transmittance properties of the samples. The transmission studies were performed in the wavelength range of 200 - 1200 nm. The direct optical band gap (E_g) was obtained by optical absorption measurements and plotting $(\alpha h\nu)$ versus photon energy ($h\nu$) and using the following relation:

$$(\alpha h\nu)^2 = A (h\nu - E_g) \quad (5)$$

Where α is the absorption coefficient, A and E_g are the constant and direct band gap of the material respectively.

3. Results and discussion

3.1. Structural properties XRD

Figure 2 shows the X-ray diffraction patterns of undoped CuO thin films sprayed at different molar concentration of copper (II) chloride dehydrate ($\text{CuCl}_2 \cdot 2\text{H}_2\text{O}$) in the starting solution. The intensity of XRD peaks was related to many factors, which include crystallization quality, density, and thickness of thin films. According to this figure the presence of sharp peaks were shown in all diffractograms and reveals that the sprayed CuO thin films are polycrystalline in nature. Two highly intense diffraction peaks observed at values of $2\theta = 35.6^\circ$ and 38.70° with a preferred orientation respectively along the (-111) and (111) axis and which can be indexed as monoclinic structured CuO, are present for all samples. These observed diffraction peaks in the recorded XRD pattern agrees well with the values available in the JCPDS card No. 80-1917 for monoclinic CuO structure.

According to the same figure it was also found that an increase in the copper chloride dehydrates ($\text{CuCl}_2 \cdot 2\text{H}_2\text{O}$) molar concentration resulted in an increase in the intensity of the two peaks. The increase in peak intensity indicates an improvement in the crystallinity of the films with increase in grain size which was demonstrated and confirmed by AFM measurement.

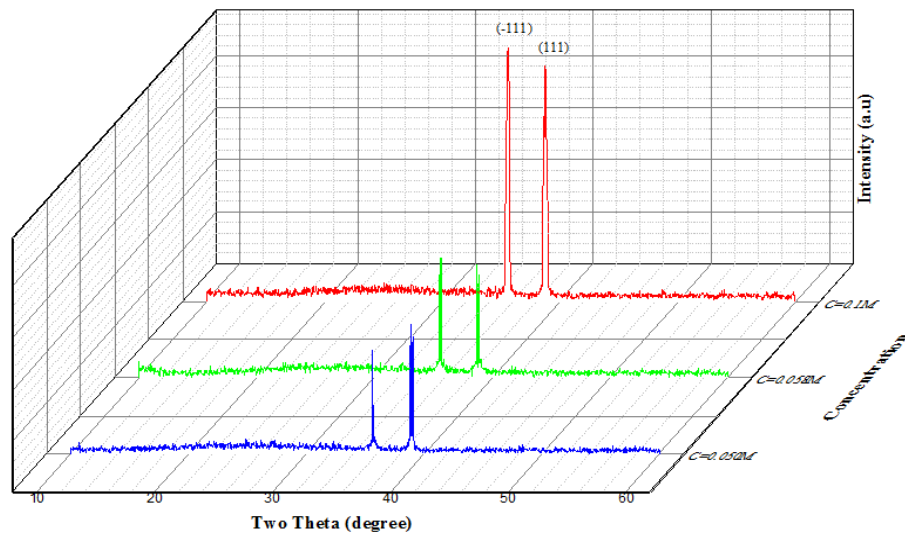


Figure 2: XRD diffractograms of Undoped CuO sprayed thin films deposited at 350 °C

The lattice parameters calculated were illustrated in the table below:

Table 1: Lattice parameters of undoped CuO thin films at different molar concentration

C (mol/l)	d_{111} (nm)	a (nm)	b (nm)	c (nm)
0.100	0.252	0.479	0.336	0.523
0.058	0.252	0.479	0.336	0.523
0.050	0.251	0.469	0.342	0.513

3.2. Morphological properties AFM

Morphological properties of the undoped CuO thin films sprayed with different molar concentrations were studied by using Atomic Force Microscopy method (AFM). According to the images below, the results obtained by AFM indicate qualitatively and quantitatively how the surface properties (topography, roughness) vary with the molar concentration of the copper chloride dehydrate ($\text{CuCl}_2, 2\text{H}_2\text{O}$). Roughness data were obtained from the recorded images using the operating software Gwyddion.

The polycrystalline nature of the sprayed CuO thin films is clearly observable in all cases. Indeed, according to the figure 3 we can see that the AFM analysis reveals the formation of micro granular particles with pyramidal shapes and irregular grain sizes, which are substantially affected by the variation of the molar concentration. From these images, it was also observed that the growth of larger grains leads to an increase in the surface roughness.

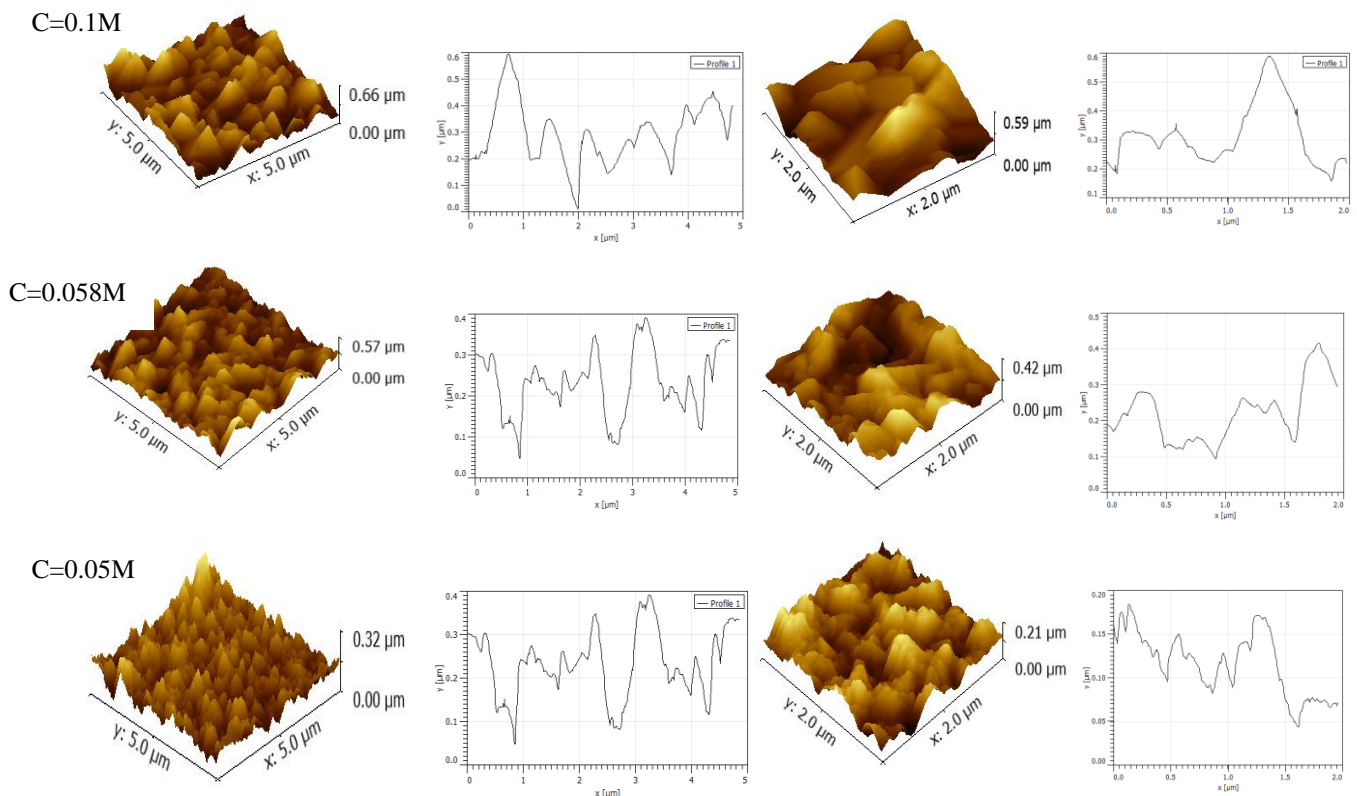


Figure 3: AFM Image of undoped CuO thin films sprayed with different molar concentration

The variations values of the average grain size as function of molar concentration were listed in below table 2.

Table 2: Average grain size at different molar concentration

Molar concentration of ($\text{CuCl}_2, 2\text{H}_2\text{O}$)	Average grain size value (μm)
0.100	0.5 – 1
0.058	0.25 – 0.5
0.050	0.1 – 0.15

With AFM images the Rms and Ra roughness parameters in function of molar concentration were deduced for these images and the values were given in the following table 3.

We observe that the RMS and Ra roughness increases with the concentration of Copper (II) chloride dehydrate ($\text{CuCl}_2, 2\text{H}_2\text{O}$).

Table 3: RMS and Ra roughness for different concentrations of undoped CuO

C (mol/l)	0.050	0.058	0.100
RMS (nm)	27	57	72
Ra (nm)	34	70	90

3.3. Optical properties

Optical transmission properties were studied within the wavelength range of 350 to 1200 nm for all sprayed CuO thin films. Figure 4 depicts the variation of this transmission as functions of molar concentration of dehydrate copper (II) chloride in the starting solution. According to this figure we observe that transmission value decreases with increase in the molar concentration. This result was attributed to the increase in film thickness.

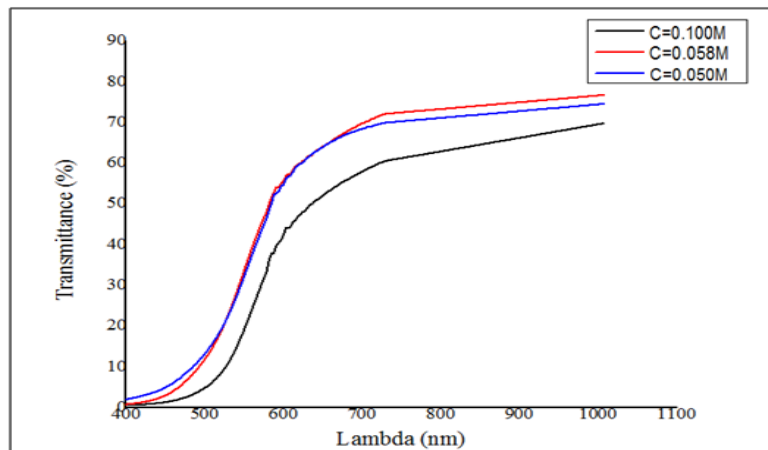


Figure 4: Optical transmission of Undoped CuO

The analysis of α in the visible region permit the energy gap calculation by lineal fit of $(\alpha h\nu)^2 = f(h\nu)$. The intercept of the tangent to the plot will give a good approximation of the band gap energy for this direct band gap material.

The band gap energy corresponding to the undoped CuO sprayed films elaborated with molar concentration of $C = 0.100M$, $C = 0.058M$ and $C = 0.050M$ is respectively about 1.29 eV, 1.39 eV and 1.47 eV as shown in the figure below. It deduce that the band gap energy decrease with increasing the molar concentration value.

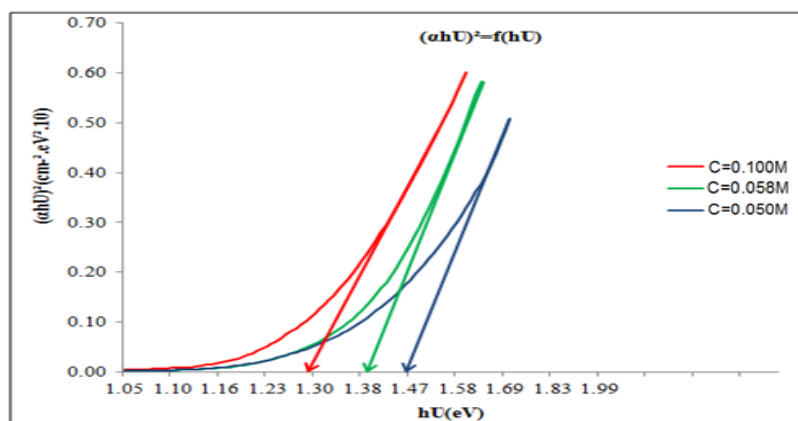


Figure 5: Band gap of Undoped sprayed CuO at different concentrations

Conclusion

Undoped CuO thin films were prepared by using a simple and low cost spray pyrolysis technique. Structural, morphological and optical properties were investigated. The obtained results reveal that the molar concentration of copper (II) chloride hydrate ($CuCl_2 \cdot 2H_2O$) in the starting solution has an influential role on the sprayed CuO thin films properties. A molar concentration of 0.1M was found to be optimum for preparing CuO thin films.

The XRD confirmed a monoclinic structure with a preferred orientation respectively the (-111) and (111) axis. It was also observed that the grain size and the surface roughness have a direct dependence of molar concentration of the precursor in the starting solution. The films transmission is around 60 - 70% in the visible zone and the optimum band gap is about 1.29 eV which is in good agreement with those published in literature. In order to improve the crystallinity of the sprayed CuO thin films, we will focus our future studies on the heat treatment under various atmospheres.

In conclusion and according to our results, we can confirm that the spray pyrolysis [30] technique is a well polystructured thin-film preparation method with excellent features.

References

1. Mugwang'a F.K., Karimi P.K., Njoroge W.K., Omayio O., Waita S.M., *Int. J. Thin Film Sci. Tec.* 2 (2013) 15–24.
2. Subramaniyan A., Perkins J. D., O'Hayre R.P., Lany S., Stevanovic V., Ginley D. S., Zakutayev A., *APL Mater.* 2 (2014) 022105.
3. Kim S.Y., Ahn C.H., Lee J.H., Kwon Y.H., Hwang S., Lee J.Y., Cho H.K., *ACS Appl. Mater. Interfaces* 5 (2013) 2417–2421.
4. Mukherjee N., Show B., Maji S.K., Madhu U., Bhar S.K., Mitra B.C., Khan G.G., Mondal A., *Mater. Lett.* 65 (2011) 3248–3250.
5. Sankar R., Manikandan P., Malarvizhi V., Fathima T., Shivashangari K.S., Ravikumar V., *Spectrochim. Acta A* 121 (2014) 746–750.
6. Umadevi M., Christy A.J., *Spectrochim. Acta A* 109(2013)133–137.
7. Sivaraj R., Rahman P.K., Rajiv P., Narendhran S., Venckatesh R., *Spectrochim. Acta A* 129 (2014) 255–258.
8. Sivaraj R., Rahman P.K., Rajiv P., Salam A.H., Venckatesh R., *Spectrochim. Acta A* 133 (2014) 178–181.
9. Samarasekara P., Kumara N.T.R.N., Yapa N.U.S., *J. Phys-Condens. Mater.* 18 (2006) 2417–2420.
10. Jundale D., Pawar S., Chougule M., Godse P., Patil S., Raut B., Sen S., Patil V., *J. Sensor Technol.* 1 (2011) 36–46.
11. Hsueh H.T., Hsueh T.J., Chang S.J., Hung F.Y., Tsai T.Y., Weng W.Y., Hsu C.L., Dai B.T., *Sensor Actuators B–Chem.* 156 (2011) 906–911.
12. Zhu G., Xu H., Xiao Y., Liu Y., Yuan A., Shen X., *ACS Appl. Mater. Interfaces* 4 (2012) 744–751.
13. Jindal K., Tomar M., Gupta V., *Biosens. Bio electron.* 38 (2012) 11–18.
14. Zhang L., Yuan F., Zhang X., Yang L., *Chem. Cent. J.* 5 (2011) 75.
15. Taubert A., Stange F., Li Z., Junginger M., Gunter C., Neumann M., Friedrich A., *ACS Appl. Mater. Interfaces* 4 (2012) 791–795.
16. Lee S., Choi S.U.S., Li S., Eastman J.A., *J. Heat Transfer* 121 (1999) 280–289.
17. Zhang Q., Zhang K., Xu D., Yang G., Huang H., Nie F., Liu C., Yang S., *Progr. Mater. Sci.* 60 (2014) 208.
18. Johan M.R., Suan M.S.M., Hawari N.L., Ching H.A., *Int. J. Electrochem. Sci.* 6 (2011) 6094–6104.
19. Sahay R., Sundaramurthy J., Suresh Kumar P., Thavasi V., Mhaisalkar S.G., Ramakrishna S., *J. Solid State Chem.* 186 (2012) 261–267.
20. Moura A.P., Cavalcante L.S., Sczancoski J.C., Stroppa D.G., Paris E.C., Ramirez A.J., Varela J.A., Longo E., *Adv. Powder Technol.* 21 (2010) 197–202.
21. Chang M. H., Liu H.S., Tai C.Y., *Powder Technol.* 207 (2011) 378–386.
22. Vidyasagar C.C., Naik Y.A., Venkatesh T.G., Viswanatha R., *Powder Technol.* 214 (2011) 337–343.
23. Mallick P., Sahu S., *Nano sci. Nanotechnol.* 2 (2012) 71–74.
24. Chiang C.Y., Shin Y., Ehrman S., *J. Electrochem. Soc.* 159 (2012) B227–B231.
25. Sathyamoorthy R., Mageshwari K., *Phys. E* 47 (2013) 157–161.
26. Jayaprakash J., Srinivasan N., Chandrasekaran P., Girija E.K., *Spectrochim. Acta A* 136 (2015) 1803–1806.
27. Bayansal F., Cetinkara H.A., Kahraman S., Cakmak H.M., Guder H.S., *Ceram. Int.* 38 (2012) 1859–1866.
28. Gao D., Yang G., Li J., Zhang J., Xue D., *J. Phys. Chem. C* 114 (2010) 18347–18351.
29. Upadhyay S., Sharma D., Singh N., Satsangi V.R., Shrivastav R., Waghmare U.V., Dass S., *J. Mater. Sci.* 49 (2014) 868–876.
30. Morales J., Sanchez L., Martin F., Ramos-Barrado J.R., Sanchez M., *Electrochim. Acta* 49 (2004) 4589.